INFECTIOUS DISEASE

Unfolded protein response inhibitors cure group A streptococcal necrotizing fasciitis by modulating host asparagine

Aparna Anand[1†], Abhinay Sharma[1†], Miriam Ravins[1], Debabrata Biswas[2,3], Poornima Ambalavanan[2,3], Kimberly Xuan Zhen Lim[2,3], Rachel Ying Min Tan[2,3], Atul Kumar Johri[4], Boaz Tirosh[5]*, Emanuel Hanski[1,2,3]*

Group A streptococcus (GAS) is among the top 10 causes of mortality from an infectious disease, producing mild to invasive life-threatening manifestations. Necrotizing fasciitis (NF) is characterized by a rapid GAS spread into fascial planes followed by extensive tissue destruction. Despite prompt treatments of antibiotic administration and tissue debridement, mortality from NF is still high. Moreover, there is no effective vaccine against GAS, and early diagnosis of NF is problematic because its clinical presentations are not specific. Thus, there is a genuine need for effective treatments against GAS NF. Previously, we reported that GAS induces endoplasmic reticulum (ER) stress to gain asparagine from the host. Here, we demonstrate that GAS-mediated asparagine induction and release occur through the PERK-eIF2α-ATF4 branch of the unfolded protein response. Inhibitors of PERK or integrated stress response (ISR) blocked the formation and release of asparagine by infected mammalian cells, and exogenously added asparagine overcame this inhibition. Moreover, in a murine model of NF, we show that the inhibitors minimized mortality when mice were challenged with a lethal dose of GAS and reduced bacterial counts and lesion size when mice were challenged with a sublethal dose. Immunohistopathology studies demonstrated that PERK/ISR inhibitors protected mice by enabling neutrophil infiltration into GAS-infected fascia and reducing the pro-inflammatory response that causes tissue damage. Inhibitor treatment was also effective in mice when started at 12 hours after infection. We conclude that host metabolic alteration induced by PERK or ISR inhibitors is a promising therapeutic strategy to treat highly invasive GAS infections.

INTRODUCTION

Streptococcus pyogenes, group A streptococcus (GAS), is a Gram-positive extracellular strict human pathogen. It is among the top 10 causes of mortality from an infectious disease (*1*, *2*). GAS strains are subclassified serologically or genetically based on the variance in the N-terminal amino acid sequences of the surface M protein, a major virulence factor encoded by the *emm* gene (*3*). More than 220 different *emm* types exist, and the GAS clone of *emm*-type M1T1 has spread globally and is one of the dominant serotypes causing diseases among the populations of industrialized countries (*4*–*6*).

Despite being sensitive to penicillin, GAS causes diverse manifestations, ranging from mild to invasive diseases with high mortality rates. GAS also causes toxin-mediated diseases like scarlet fever and streptococcal toxic shock syndrome and autoimmune sequelae such as rheumatic fever and glomerulonephritis (*2*, *7*–*13*). More than 18 million globally are estimated to suffer from serious GAS diseases, with about 1.78 million new cases annually. In addition, hundreds of millions of people develop mild GAS infections every year, placing a massive burden on health care systems (*7*, *14*).

Invasive GAS infections are defined as infections of usually sterile sites, including bacteremic pneumonia, sepsis, and necrotizing fasciitis (NF) (*13*). NF is an acute, rapidly progressive, severe deep-seated infection of the subcutaneous tissue. It begins at a site of trivial or even unapparent trauma. The initial lesion may appear only as mild erythema, but inflammation becomes extensive within a short period, leading to a destructive skin and soft tissue process over large body areas (*15*). The mainstay of treatment for invasive GAS diseases is administering antibiotics, surgical debridement of infected tissues, and supportive care (*16*). Unfortunately, regardless of prompt therapy, the associated mortality rate from NF remains high, ranging from 23 to 35% in resource-rich settings (*7*, *8*, *10*, *11*, *13*, *17*). Because there is no effective vaccine against GAS (*18*, *19*), there is an urgent need for approaches to combat invasive soft tissue GAS infections.

We have previously isolated a cluster of strains from NF GAS infections in Israel (*20*). Using a strain from this cluster, we developed a mouse model mirroring human GAS soft tissue infection. The infection was histologically characterized by the destruction of soft tissue, paucity of infiltrating phagocytes, and the presence of a large number of Gram-positive cocci at the fascial plane (*15*, *21*). By using this model, we demonstrated that GAS induces endoplasmic reticulum (ER) stress and consequently triggers the unfolded protein response (UPR) (*22*). These processes provide extracellular asparagine for the bacteria. Furthermore, asparagine is sensed by GAS, causing a transcription alteration of 17% of GAS genes and increasing bacterium multiplication rate (*22*). Nevertheless, the signaling pathways of UPR responsible for the GAS-mediated generation of asparagine remained unidentified.

The integrated stress response (ISR) is a cellular signaling network that couples the detection of cellular stresses to the inhibition

[1]Department of Microbiology and Molecular Genetics, The Institute for Medical Research, Israel-Canada (IMRIC), Faculty of Medicine, The Hebrew University of Jerusalem, Jerusalem 9112102, Israel. [2]Singapore-HUJ Alliance for Research and Enterprise, MMID Phase II, Campus for Research Excellence and Technological Enterprise (CREATE), Singapore 117576, Singapore. [3]Department of Microbiology and Immunology, National University of Singapore, Singapore 138602, Singapore. [4]School of Life Sciences, Jawaharlal Nehru University, New Mehrauli Road, New Delhi 110067, India. [5]Institute for Drug Research, School of Pharmacy, Faculty of Medicine, The Hebrew University of Jerusalem, Jerusalem 9112102, Israel.
*Corresponding author. Email: emanuelh@ekmd.huji.ac.il (E.H.); boazt@ekmd.huji.ac.il (B.T.)
†These authors contributed equally to this work.

of translation initiation by phosphorylating the α subunit of the eukaryotic translation initiation factor (eIF2α) at Ser^{51} to elicit a transcriptional and translational stress response (*23*–*26*). ISR includes conditions leading to a buildup of misfolded proteins in the ER, a condition called ER stress. Three ER transmembrane proteins sense ER stress: protein kinase RNA (PKR)–like ER kinase (PERK), activating transcription factor 6 (ATF6), and inositol-requiring protein 1 (IRE1). Upon sensing stress, these sensors trigger the UPR (*27*). The PERK branch of UPR leads to the ATF4. ATF4 controls the expression of a range of adaptive genes involved in cellular recovery, including asparagine synthetase (*28*). This signaling pathway of UPR is termed as PERK-eIF2α-ATF4 pathway (*27*, *29*). GSK2606414 and GSK2656157 are selective PERK inhibitors, and the latter was selected for preclinical development (*30*). The ISR-mediated phosphorylation of eIF2α (p-eIF2α) inhibits eIF2B, the guanine nucleotide exchange factor that recycles inactive eIF2–guanosine diphosphate (GDP) to active eIF2–guanosine triphosphate (GTP). A small-molecule ISR inhibitor (ISRIB) rescues translation in the presence of p-eIF2α by facilitating the assembly of more active eIF2B (*31*, *32*).

Because we identified that GAS activates the PERK-eIF2α-ATF4 pathway specifically to obtain asparagine from the host, we set out to examine whether inhibitors of this pathway could treat GAS invasive infections. We demonstrate that the inhibitors cure invasive GAS soft tissue infections in a murine model.

RESULTS

GAS induces asparagine production in host cells via the PERK-eIF2α-ATF4 pathway

To identify the host UPR pathways targeted by GAS to increase asparagine availability for its benefit, we used HaCaT human keratinocyte cells relevant to GAS infection (*33*). HaCaT cells were infected with GAS strain JS12 harboring the P4 promoter of *sil* (streptococcal invasion locus) fused to *gfp* (JS12p*P4-gfp*). *sil* is a quorum-sensing system that is activated by the autoinducer peptide SilCR, as illustrated in fig. S1A. JS12 has an intact *sil* locus that senses asparagine and consequently activates *sil* P3, P4, and P6 promoters to a threshold degree (*34*); these promoters are then further activated by the autoinduction process producing SilCR. JS12p*P4-gfp* produces green fluorescent protein (GFP) when *sil* is activated and thus serves as a reporter for extracellular asparagine in the medium (*22*, *34*). P4 promoter activity was enhanced during infection of HaCaT cells by JS12p*P4-gfp*, as determined by the mean fluorescence intensity (MFI) of GFP using flow cytometry (Fig. 1, A and B). GFP accumulation was time dependent and inhibited in a dose-dependent manner by the specific inhibitor of PERK, GSK2606414 (Fig. 1A) (*30*). Because GSK2606414 did not affect GAS growth in vitro (fig. S1B), these results suggested that the GAS-mediated induction of host asparagine production occurs via activation of the PERK-eIF2α-ATF4 pathway. Similarly, the addition of ISRIB did not affect GAS growth in vitro (fig. S1C) but inhibited GFP accumulation in JS12p*P4-gfp*–infected HaCaT cells in a dose-dependent manner (Fig. 1B). These findings further favor the notion that GAS activates the PERK-eIF2α-ATF4 pathway and that inhibitors of this pathway's components block asparagine formation.

To demonstrate that the production of asparagine through the PERK-eIF2α-ATF4 pathway is independent of the presence or the absence of an active *sil* (which is used here solely as a reporter), we infected HaCaT cells with four strains of GAS of two different M types, which neither possess (854, 5448, of M1T1 type) nor have a functional *sil* (JS14, JS95, of M-14 type). We collected the culture media and assessed their asparagine content at the indicated times after infection by applying the indirect *sil* activation assay described previously (*22*). In this assay, GAS strains that do not have active *sil* are first incubated with mammalian cells, and the culture media (free of cells and bacteria) are collected and further incubated with the reporter strain JS12p*P4-gfp* to assess the asparagine content. Irrespective of their M types, the four strains induced asparagine formation and release from HaCaT cells in a time-dependent manner, and asparagine formation and release were blocked by GSK2606414 (fig. S1D). Next, we demonstrated that exogenously added asparagine overrode the inhibitory effect of GSK2606414 in GAS-infected HaCaT cells (Fig. 1C). Both PERK inhibitors, GSK2606414 and GSK2656157 (*30*), prevented *sil* activation in GAS-infected HaCaT cells, and the inhibition was reversed by adding 10 or 100 μg/ml of exogenous asparagine (fig. S1, E and F). We also performed similar experiments with mouse embryonic fibroblasts (MEFs) and obtained comparable results; GSK2606414 inhibited *sil* activation, and the inhibition was alleviated by adding exogenous asparagine (fig. S1G). Because incubation with host cells enhances GAS growth (*22*, *34*), we enumerated colony-forming units (CFUs) as a function of time after infection of HaCaT cells with JS12. Whereas GSK2606414 did not affect GAS growth in vitro (fig. S1B), it inhibited GAS growth in the presence of HaCaT cells and exogenously added asparagine ameliorated GAS growth inhibition by GSK2606414 (Fig. 1D). JS12 has an intact *sil* but does not cause invasive infection in a murine model of human NF. For this infection model, we used GAS strain JS14 isolated from a collection of invasive GAS infections reported in Israel (*20*). To ensure that JS14 growth behavior on HaCaT cells was similar to that of JS12, we grew JS14 on HaCaT cells and found that GSK2606414 inhibited JS14 growth, and the inhibition was alleviated by the addition of exogenous asparagine (fig. S1H).

Next, we measured the transcript amounts of *atf4* and asparagine synthetase (*asns*) in HaCaT cells infected by JS12 strain in the presence or absence of GSK2606414 or ISRIB. Transcript amounts of both genes were significantly up-regulated upon GAS infection ($P = 0.0002$ for *atf4* and $P \leq 0.0001$ for *asns*) in a time-dependent manner, and their expression was significantly ($P \leq 0.05$) repressed in the presence of either of the inhibitors (Fig. 1, E and F). Similar results were generated for MEF cells when infected with GAS strain JS12 or HaCaT cells when infected with 5448 (serotype M1T1) (fig. S1, I to L). We then performed Western blot analyses to assess the phosphorylation amounts of PERK and eIF2α in HaCaT cells infected with GAS in the presence or absence of GSK2606414 or ISRIB. HaCaT cells, infected with strain JS12, displayed increased PERK and eIF2α phosphorylation (Fig. 1G). In addition, increased phosphorylation of PERK upon GAS infection was observed for all the different GAS strains tested (fig. S1M). Also, GSK2606414 but not ISRIB (which acts downstream) inhibited GAS-induced increased phosphorylation of PERK and eIF2α, and both were phosphorylated when cells were incubated with thapsigargin (TG) (Fig. 1G). Thus, GAS uses the PERK-eIF2α-ATF4 pathway of the UPR to generate the asparagine required by the bacterium, and the two other arms of the UPR do not contribute to the effect. The IRE1-XBP1 pathway inhibitor, STF-083010 (*35*), and the inhibitor of the ATF6 pathway, AEBSF (*36*), inhibited mRNA expression of spliced *xbp1* or *ERp72*, respectively, when UPR was induced in

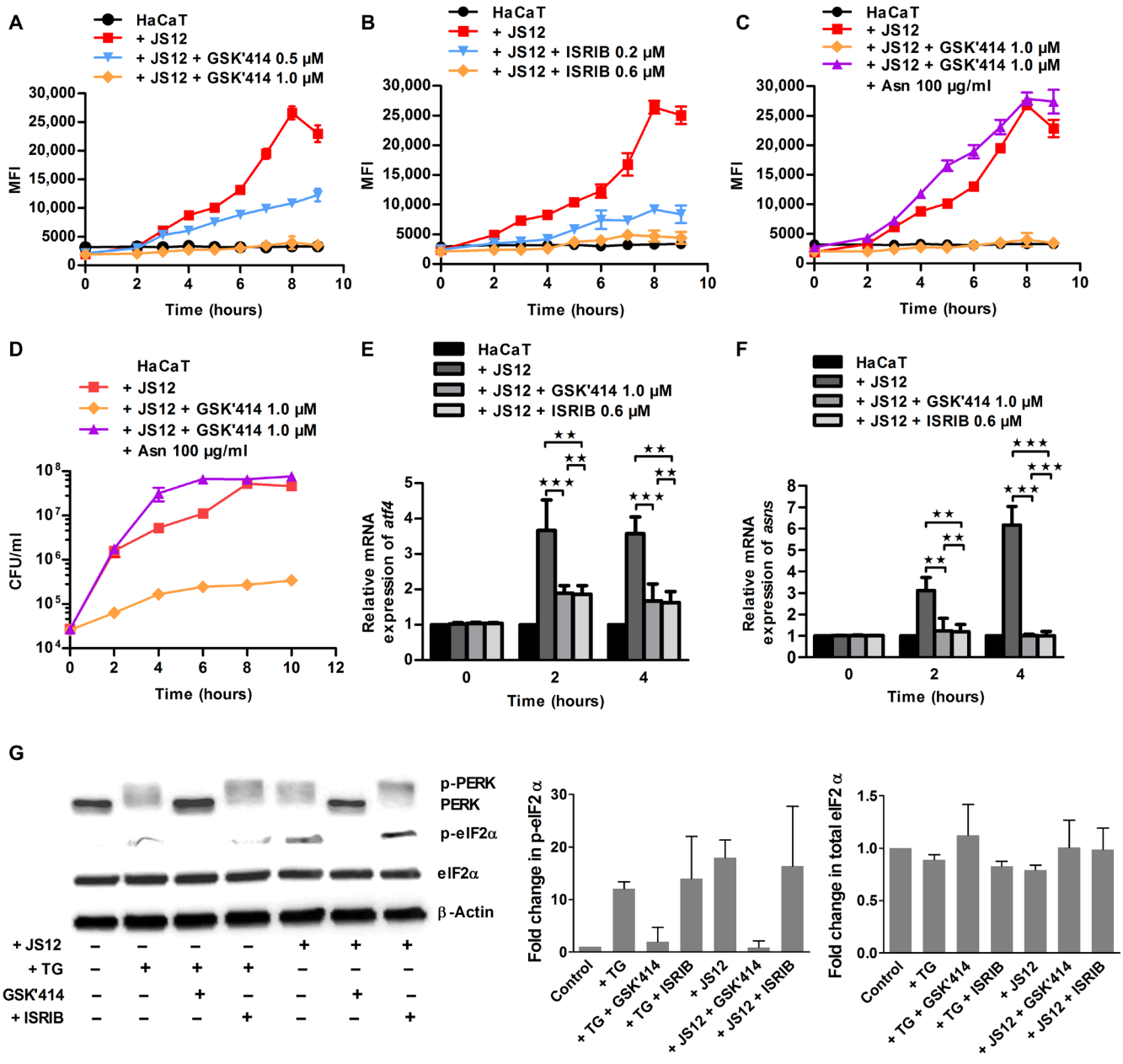

Fig. 1. GAS activates the PERK-eIF2α-ATF4 pathway to acquire asparagine from HaCaT cells. (**A** to **C**) Quantification of *sil* activation upon acquisition of asparagine from HaCaT cells. HaCaT cells were infected with GAS strain JS12, harboring the plasmid p*P4-gfp* (JS12p*P4-gfp*) at multiplicity of infection (MOI) = 1. Mean fluorescence intensity (MFI) representing GFP accumulation was determined by flow cytometry (FACS). (A and B) Dose-dependent inhibition of GSK2606414 and ISRIB on *sil* activation. (C) Asparagine (Asn) addition reversed GSK2606414-mediated inhibition of *sil* activation. The values shown are the mean of three determinations ± SD in a single experiment. Two independent experiments were performed and yielded similar results (table S1). (**D**) Quantification of bacterial CFU per ml at different time intervals when incubated with HaCaT cells at MOI = 1 in the presence or absence of GSK2606414. The values shown are the mean of two determinations ± SD (table S1). (**E** and **F**) Real-time RT-PCR of activating transcription factor 4 (*atf4*) and asparagine synthetase (*asns*) genes in HaCaT cells infected with JS12p*P4-gfp* in the presence and absence of GSK2606414 and ISRIB. HaCaT cells were infected with JS12p*P4-gfp* strain at MOI = 1 in the presence or absence of GSK2606414 or ISRIB. (E) *atf4* and (F) *asns* transcript abundance was determined by real-time RT-PCR after 2 and 4 hours of incubation and normalized to the transcript abundance of β-actin. The amounts of the corresponding transcript in uninfected cells were designated as 1. The real-time RT-PCR for each sample was performed in triplicates, and the values shown represent the means ± SEM. One-way ANOVA with Tukey post-test, $^{**}P < 0.01$; $^{***}P < 0.001$. (**G**) Western blot analysis of UPR markers in GAS-infected HaCaT cells. HaCaT cells were incubated with thapsigargin (TG) (0.25 μM) or infected with JS12p*P4-gfp* at MOI = 1 for 4 hours at 37°C in the absence or presence of GSK2606414 (1 μM) or ISRIB (0.6 μM). Cells were then harvested, lysed, and subjected to SDS–polyacrylamide gel electrophoresis followed by Western blot analysis. β-Actin was used as a loading control. Quantification of p-eIF2α and total eIF2α was performed using ImageJ software.

HaCaT cells by TG. However, when UPR was induced by GAS infection, the mRNA amounts of spliced *xbp1* or *ERp72* remained the same as in the noninfected HaCaT cells (fig. S1, N and O). Collectively, these findings show that GAS-induced asparagine formation in mammalian cells is mediated by activating the PERK-eIF2α-ATF4 pathway.

Asparagine affects GAS growth and expression of *mga*, *emm*, and *scpA* genes

In a recent study, we assessed the effect of asparagine on GAS global gene expression by growing the bacteria in a Todd-Hewitt broth with yeast extract (THY) medium supplemented with recombinant asparaginase from *Erwinia chrysanthemi* (Kidrolase), which hydrolyzes asparagine and serves as an anticancer chemotherapy drug (*22*, *37*). Nevertheless, Kidrolase generates toxic effects on eukaryotic cells (*37*) and may alter the metabolism of GAS due to a constant depletion of asparagine from the medium. Therefore, we tested the effect of asparagine on GAS growth and gene expression in a chemically defined medium (CDM) that lacks asparagine, with asparagine supplemented at controlled concentrations. The growth curves of M-14 type strains (JS14 and JS95) (Fig. 2, A and B) isolated from patients with invasive GAS diseases in Israel (*20*) and M1T1 strains 854 and 5448 (Fig. 2, C and D) show that exogenously added asparagine increased the growth rate significantly ($P \leq 0.0001$) at a concentration of 10 μg/ml. We also tested GAS dependence on asparagine using additional M1T1 strains (AP1, MGAS 5005, and GAS 2008-119) and found that all strains tested exhibited a higher growth rate in the presence of asparagine (fig. S2, A to C).

We tested the influence of asparagine on the transcription of few virulence genes in GAS grown in CDM. The results demonstrate that exogenously added asparagine at 10 μg/ml strongly up-regulated the transcription of *mga*, *emm*, and *scpA* compared to CDM without asparagine. This trait was found for JS14 (Fig. 2E), JS95 (fig. S2D), used by us previously (*22*), and strain 5448 (Fig. 2F). Mga is a standalone response regulator controlling global virulence networks in GAS (*38*), including the operon, Mga itself, M protein, C5a peptidase–ScpA, and other genes involved in the regulation of metabolism (*39*, *40*). These results demonstrate that asparagine may affect bacterial virulence due to transcription up-regulation of *mga* and, consequently, GAS genes encoding critical virulence factors such as M protein and ScpA (*3*, *41*, *42*).

Last, to demonstrate that the transcription of the indicated virulence factors occurs ex vivo in the context of the PERK-eIF2α-ATF4 pathway, we measured the transcript amounts of *mga*, *emm*, and

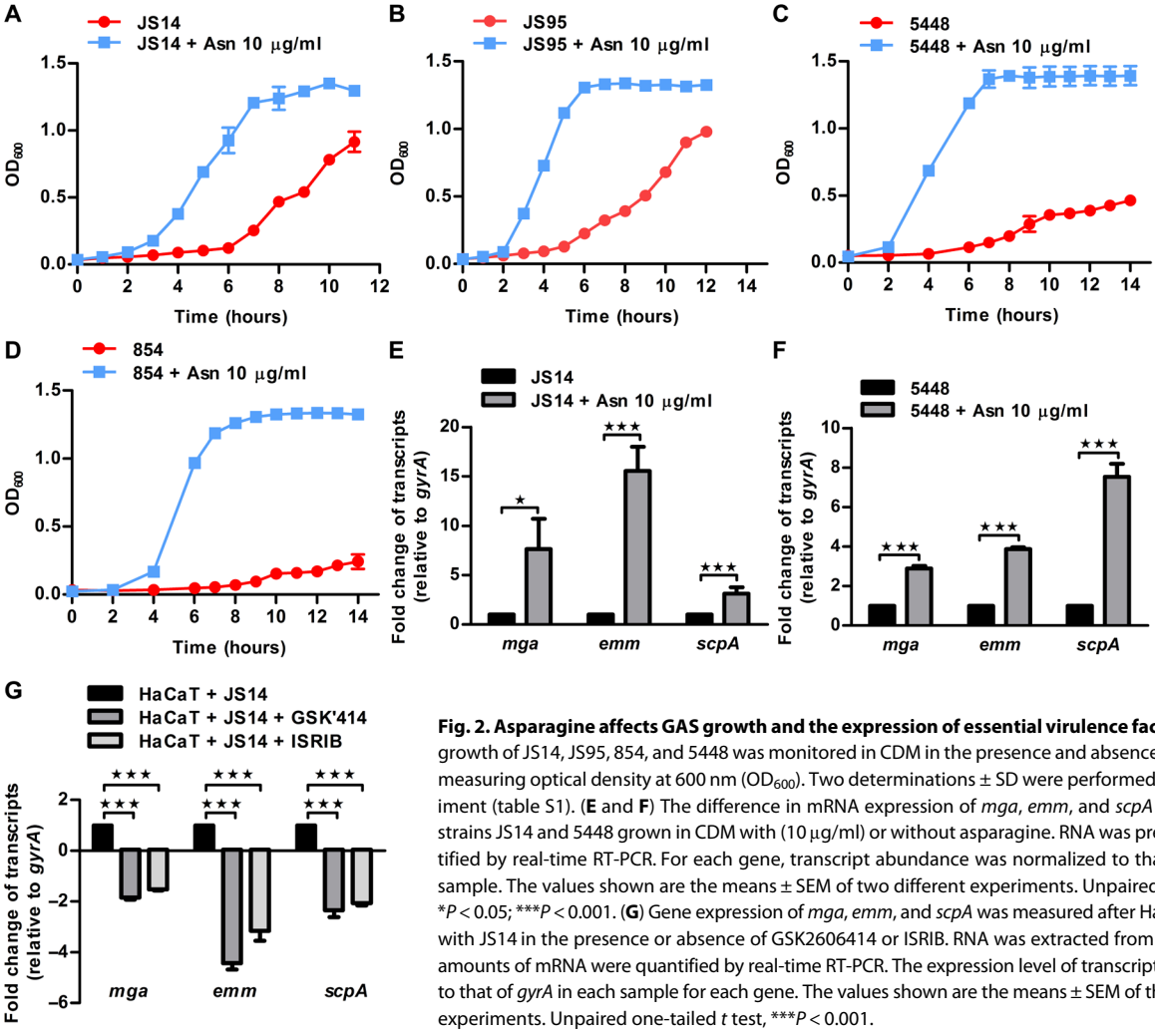

Fig. 2. Asparagine affects GAS growth and the expression of essential virulence factors. (**A** to **D**) The growth of JS14, JS95, 854, and 5448 was monitored in CDM in the presence and absence of asparagine by measuring optical density at 600 nm (OD_{600}). Two determinations ± SD were performed in a single experiment (table S1). (**E** and **F**) The difference in mRNA expression of *mga*, *emm*, and *scpA* was measured in strains JS14 and 5448 grown in CDM with (10 μg/ml) or without asparagine. RNA was prepared and quantified by real-time RT-PCR. For each gene, transcript abundance was normalized to that of *gyrA* in each sample. The values shown are the means ± SEM of two different experiments. Unpaired one-tailed *t* test, $^{*}P < 0.05$; $^{***}P < 0.001$. (**G**) Gene expression of *mga*, *emm*, and *scpA* was measured after HaCaT cell infection with JS14 in the presence or absence of GSK2606414 or ISRIB. RNA was extracted from bacteria, and the amounts of mRNA were quantified by real-time RT-PCR. The expression level of transcripts was normalized to that of *gyrA* in each sample for each gene. The values shown are the means ± SEM of three independent experiments. Unpaired one-tailed *t* test, $^{***}P < 0.001$.

scpA in JS14 incubated with HaCaT cells for 6 hours under similar conditions to those used for *sil* activation in JS12. There was a decrease in the expression of the indicated genes in the presence of GSK2606414 and ISRIB (Fig. 2G). These results confirm that the transcription of *mga*, *emm*, and *scpA* is affected by PERK-eIF2α-ATF4 pathway inhibitors during infection with host cells.

GSK2656157 and ISRIB protect mice against GAS infections

Because asparagine acquisition by GAS occurs in vivo in the murine model of human soft tissue infection (*22*), we tested whether PERK-eIF2α-ATF4 pathway inhibitors would protect mice against infection with a lethal dose of GAS. For this purpose, we subcutaneously challenged BALB/c mice with 1.5×10^8 CFU of JS14. Infected mice were treated for 5 days after infection by repeated subcutaneous and intraperitoneal injections of the PERK inhibitor GSK2656157. The Kaplan-Meier survival analysis showed that mortality rates in infected mice treated with GSK2656157 were significantly ($P = 0.0014$) lower compared to untreated infected mice ($n = 15$ per group). Moreover, at 14 days after infection, mouse survival in the GSK2656157-treated group was 80%, whereas only 30% of the untreated mice survived (Fig. 3A). ISRIB treatment was also equally effective at increasing survival in mice challenged with a lethal dose of JS14 (Fig. 3B), suggesting that inhibitors acting along the PERK-eIF2α-ATF4 pathway axis protect against GAS infection. In addition, treatment with GSK2656157 completely prevented mouse mortality when mice were challenged with strain 5448, whereas 50% of the mice died in the untreated infected group within 14 days after infection (Fig. 3C).

To follow the bacterial burden of GAS strain 5448 in surviving mice, we enumerated CFUs in soft tissue at day 3 after infection from both GSK2656157-treated and untreated mice and found that they contained a comparable count of bacterial colonies (2×10^{10} CFU per gram of tissue). CFUs in soft tissue from GSK2656157-treated mice started showing a decline at day 6 after infection and were two to three orders of magnitude lower at day 10 and almost seven orders of magnitude lower on day 14 after infection (Fig. 3D). Furthermore, the CFUs recovered from the spleen of GSK2656157-treated mice were significantly lower at days 10 and 14 after infection ($P = 0.0079$ and 0.0109, respectively) than in untreated mice (fig. S3A). GSK2656157 treatment may affect glucose-stimulated insulin secretion (*43*); however, we did not observe a significant ($P > 0.05$) change in the body weight of GSK2656157-treated versus untreated mice (fig. S3B). In addition, mice treated with GSK2656157 displayed smaller lesions during the infection than the untreated mice (Fig. 3E and fig. S3C), indicating improved local and systemic recoveries.

GSK2656157 acts by enhancing neutrophil-mediated GAS clearance

We reasoned that infecting mice with a lethal dose ($\geq 1 \times 10^8$ CFU) of GAS could overwhelm the immune system and trigger responses

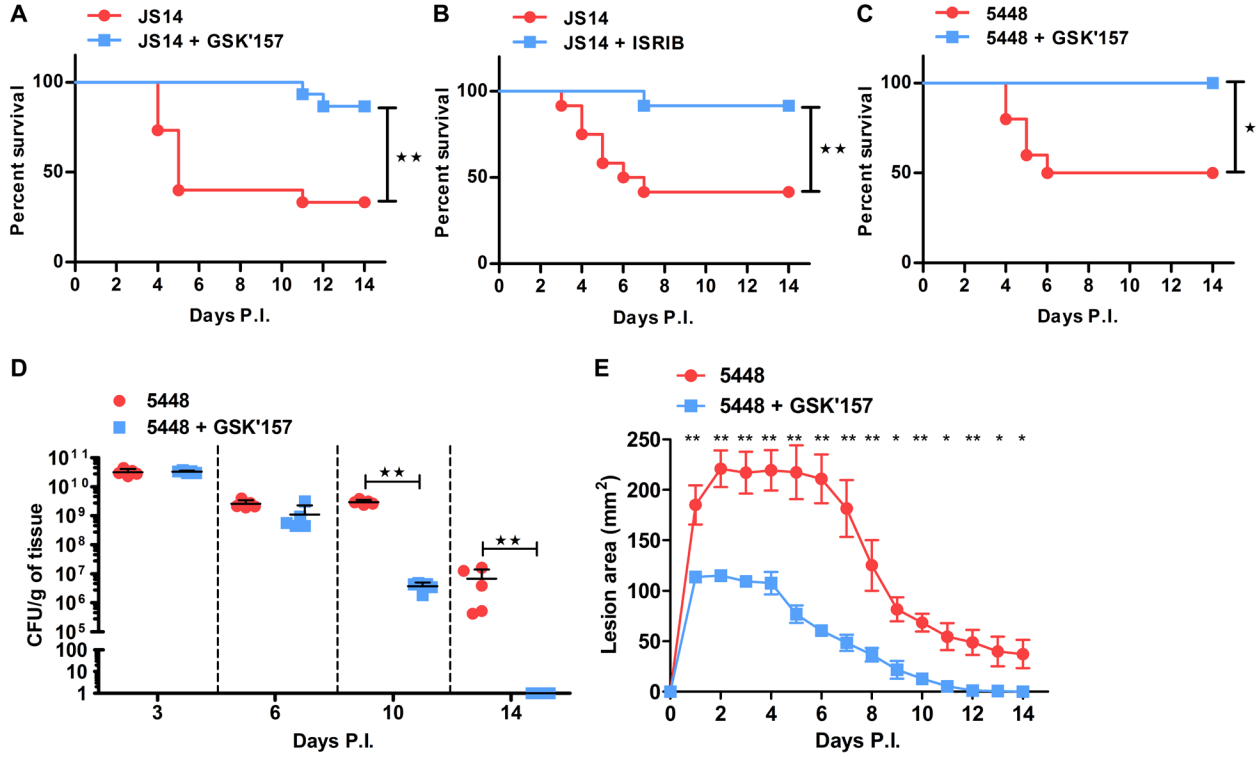

Fig. 3. GSK2656157 and ISRIB protect mice against GAS lethal soft tissue infections. (**A** to **C**) Kaplan-Meier survival analysis of BALB/c mice [(A and C), $n = 15$ per group; (B), $n = 12$ per group] infected by subcutaneous administration of 1.5×10^8 CFU of strain JS14 (A and B) or 2.5×10^8 CFU of strain 5448 (C) and subsequently untreated or treated for 5 days post-infection (P.I.) with GSK2656157 (A and C) or with ISRIB (B). Log-rank (Mantel-Cox) test for indicated treatments compared to the corresponding untreated mice; $^{**}P < 0.01$; $^{*}P < 0.05$. (**D**) Data represent CFU counts per gram of soft tissue, derived after infection from mice ($n = 5$ per group) infected with 2.5×10^8 CFU of strain 5448 and untreated or treated with GSK2656157. Data are means ± SD. Mann-Whitney *U* test, $^{**}P < 0.01$. (**E**) Skin lesion sizes in mice ($n = 5$ per group) infected with 2.5×10^8 CFU of strain 5448 and subsequently untreated or treated with GSK2656157. The lesion area (mm^2) was measured using a digital caliper. Data are means ± SD. Mann-Whitney *U* test, $^{*}P < 0.05$; $^{**}P < 0.01$.

that are not strictly relevant to human GAS infection. Therefore, we infected mice subcutaneously with a sublethal dose of 5×10^6 CFU of JS14 and monitored lesion size and enumerated CFUs in the soft tissue and spleen. Mice developed lesions with sizes peaking around day 4 after infection, and lesions were visible for up to 14 days after infection (Fig. 4, A and B). However, from days 6 to 8 after infection, a slight decrease in CFU was observed in mice soft tissue from the untreated infected group, and their spleens showed significant ($P \leq 0.0195$) bacterial accumulation (Fig. 4, C and D). In addition, treatment of mice with GSK2656157 caused a marked reduction of GAS CFUs in soft tissue and spleen (Fig. 4, C and D) and prevented spleen increase compared to the untreated mice (fig. S4A).

Neutrophils are the primary host innate immune defense against GAS infections (*13*, *44*). Therefore, we examined GAS and neutrophil distribution in infected soft tissue by immunohistopathology. On day 2 after infection, GAS and neutrophil distributions in tissue

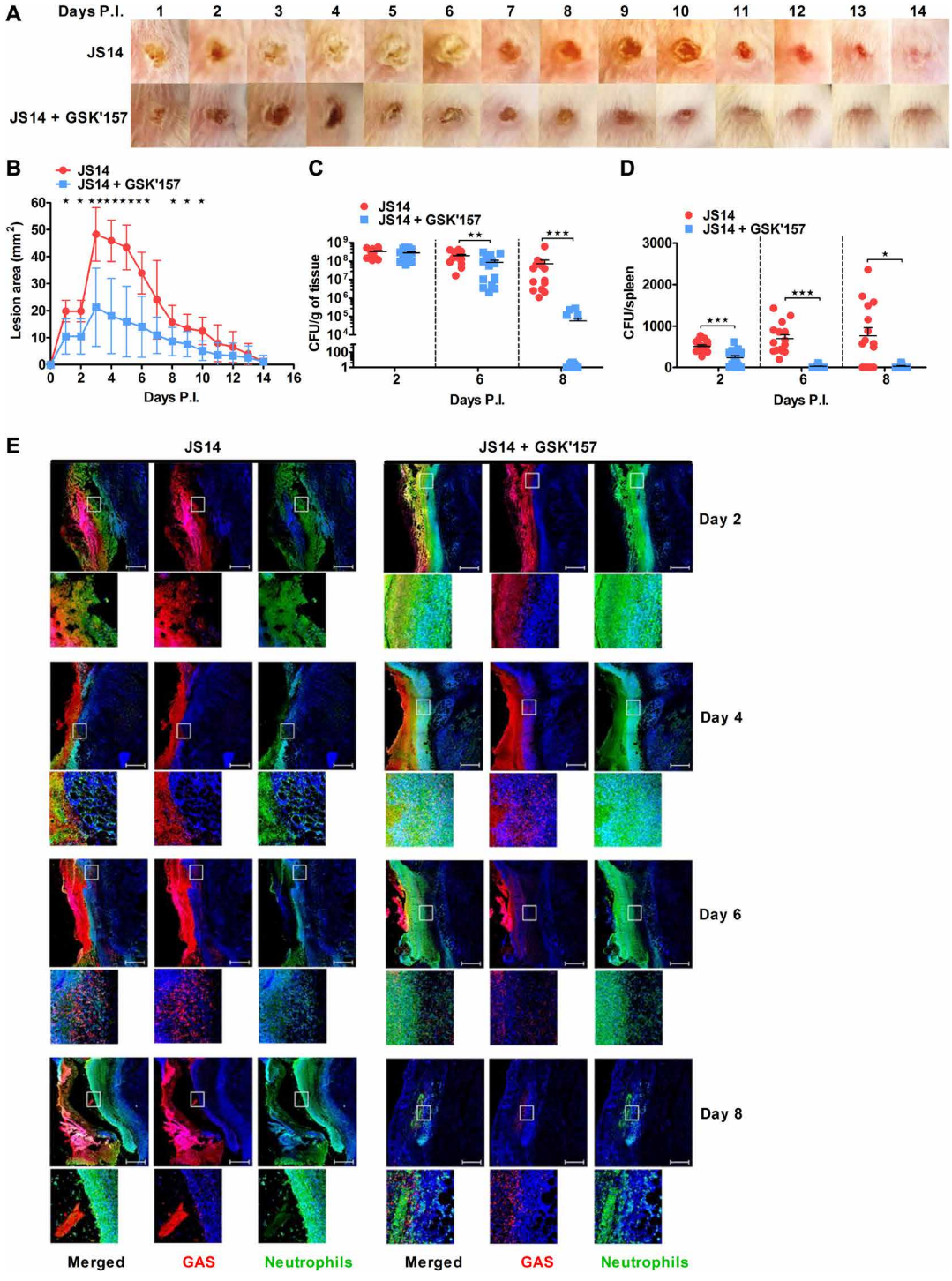

Fig. 4. GSK2656157 clears GAS soft tissue infection by enhancing the infiltration of neutrophils. BALB/c mice were infected by subcutaneous administration of 5×10^6 CFU (a sublethal dose) of strain JS14 and then were either untreated or treated for 5 days after infection with GSK2656157. (**A**) Representative images of skin lesions in untreated and GSK2656157-treated mice at indicated times after infection. (**B**) GSK2656157-treated or untreated groups of BALB/c mice ($n = 5$ per group) were injected subcutaneously with a sublethal dose (5×10^6 CFU) of JS14 strain, and lesion size was measured using a digital caliper daily up to 14 days after infection. Data are means ± SD. Unpaired one-tailed *t* test, $^*P < 0.05$; $^{**}P < 0.01$. (**C**) Data represent CFU counts per gram of soft tissue derived from GSK2656157-treated or untreated mice ($n = 15$ per group) after subcutaneous infection. Data are means ± SEM. Mann-Whitney *U* test, $^*P < 0.05$; $^{**}P < 0.01$; $^{***}P < 0.001$. (**D**) CFU counts per spleen, derived from GSK2656157-treated or untreated mice ($n = 15$ per group) after subcutaneous infection. Data are means ± SEM. Mann-Whitney *U* test, $^*P < 0.05$; $^{***}P < 0.001$. (**E**) Representative micrographs of mouse soft tissue biopsies collected from GSK2656157-treated or untreated mice after subcutaneous infection with JS14 at indicated times after infection. The following reagents were used for immunostaining: GAS, anti–group A carbohydrate, red; neutrophils, anti–Ly-6G antibodies, green; nucleated cells, 4′,6-diamidino-2-phenylindole, blue. Scale bars, 500 μm.

sections from GSK2656157-treated and untreated mice started to show noticeable differences (Fig. 4E). Bacteria densely populated the fascial zone, with a small number of neutrophils in the untreated fascia, whereas in GSK2656157-treated mice, neutrophils entered into the bacterial-occupied fascia. On day 4 after infection, the difference between the two groups became even more apparent, with the beginning of bacterial clearance from the fascial zone of GSK2656157-treated mice. On day 6 after infection, an increase in the number of neutrophils was observed in the fascia of GSK2656157-treated mice, and the number of bacteria decreased considerably.

In contrast, in tissue sections of untreated mice, the fascia still contained a dense layer of bacteria. On day 8 after infection, almost no bacteria and traces of neutrophils were detected in sections of GSK2656157-treated mice, whereas in sections from untreated mice, the fascia still contained a considerably large number of bacteria. Furthermore, on days 6 and 8 after infection, skin sections from treated mice appeared to regain tissue integrity, whereas the tissues from untreated mice appeared consistently fragmented and damaged, showing loss of tissue integrity (Fig. 4E).

Because the initial treatment protocol included administration of GSK2656157, both subcutaneously and intraperitoneally, we wondered whether administration through both routes is necessary to exert the protective effect of GSK2656157. Therefore, we infected mice subcutaneously with a sublethal dose of GAS strain JS14 and treated them with GSK2656157. Treatment continued after infection for five consecutive days via either intraperitoneal or subcutaneous or both intraperitoneal and subcutaneous routes. On day 2 after infection, GAS CFU numbers in infected soft tissue were high and similar for all injection routes. However, on day 6 after infection, there was a slight decrease in GAS CFU only in mice injected via both the subcutaneous and intraperitoneal routes. This difference considerably intensified at day 8 after infection; the soft tissue of mice injected via both the intraperitoneal and subcutaneous routes had two to three orders of magnitude lower GAS CFUs than the soft tissue of mice injected via the single infection route (fig. S4B). Furthermore, only the intraperitoneal + subcutaneous injection route eliminated the bacteria from the spleen at days 6 and 8 after infection (fig. S4C). These results are consistent with the observation that GAS soft tissue infection is associated with severe vascular dysfunction (*45*), and therefore, both local and systemic injections of GSK2656157 are required to achieve effective treatment.

Reprogramming of asparagine metabolism by GSK2656157 or ISRIB allows efficient treatment of GAS infections in mice

We expected that GSK2656157 and ISRIB would act in vivo as they act ex vivo, namely, inhibiting the PERK-eIF2α-ATF4 pathway, thereby decreasing the asparagine synthetase up-regulation and preventing GAS from being fueled by host asparagine. We used the JS95$_{ATG}$ *pP4-luc* strain to test this notion. This strain causes a soft tissue infection in mice and has an intact *sil* locus (*22*). Luciferase activity was measured in biopsies of infected mice untreated or pretreated with GSK2656157 (subcutaneously + intraperitoneally). At 6 or 12 hours after infection, tissue samples were excised and homogenized, and luciferase activity was determined and normalized to sample weight and the CFU number (Fig. 5A and fig. S5A, respectively). Treatment with GSK2656157 significantly inhibited luciferase activity ($P \leq 0.0176$), demonstrating that the PERK-eIF2α-ATF4 pathway is inhibited by GSK2656157 in vivo, preventing GAS fueling by asparagine.

To test this notion further, we infected mice with a sublethal dose (5×10^6 CFU per mouse) of JS14 and provided the mice with exogenous asparagine to assess whether the protective effect of GSK2656157 would be reverted. We injected mice that had been pretreated with either GSK2656157 or ISRIB with asparagine subcutaneously and intraperitoneally alternately every 12 hours after infection until the sixth day and enumerated CFUs in soft tissue. Asparagine treatment negated the protective effect of GSK2656157 (Fig. 5B). GAS CFU in the soft tissue of asparagine-treated mice increased at days 8 and 10 after infection by about 1000- and 10,000-fold, respectively, reaching the CFUs of mice infected with JS14 (Fig. 5B). Asparagine administration also abrogated the decreased CFUs of GAS observed in the spleen of GSK2656157-treated mice by day 8 after infection (fig. S5B). Moreover, spleen's sizes of asparagine-administered

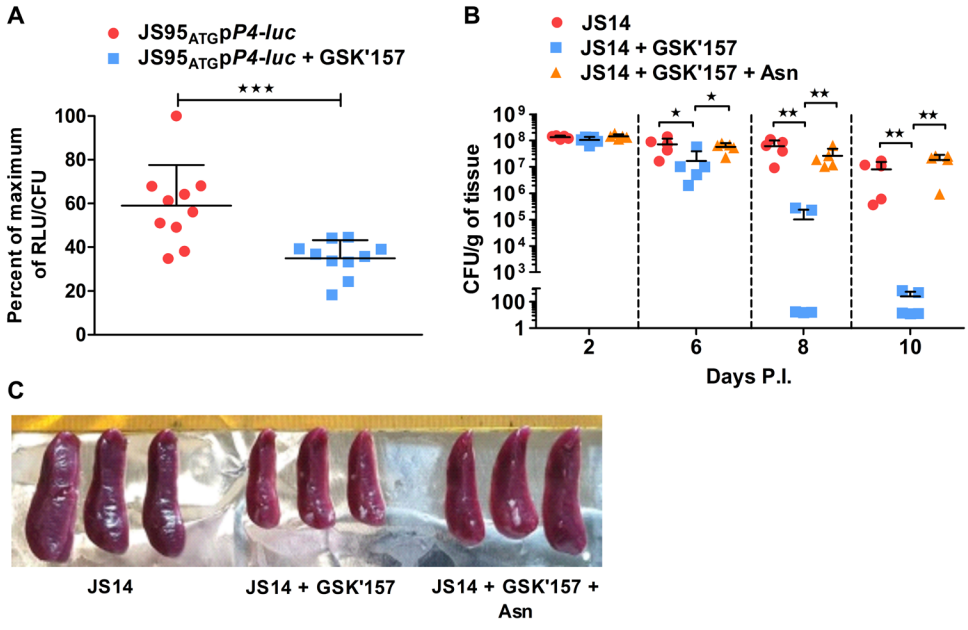

Fig. 5. GSK2656157 and ISRIB act in vivo to inhibit the reprogramming of asparagine metabolism by GAS. (**A**) BALB/c mice ($n = 10$ per group) were untreated or treated with GSK2656157 every 12 hours for 3 days before bacterial infection and infected by subcutaneous administration of 1.5×10^8 CFU (lethal dose) of strain JS95p*P4-luc*. Mice were euthanized at 6 hours after infection. Biopsies were taken and homogenized, and relative luminescence units (RLUs) were normalized to CFUs. Each value represents the mean of two determinations conducted for each punch biopsy. Unpaired one-tailed *t* test, ***$P < 0.001$. (**B**) BALB/c mice were infected by subcutaneous administration of 5×10^6 CFU (a sublethal dose) of strain JS14 and then were either untreated or treated with GSK2656157 or with GSK2656157 + Asn. Data are CFU counts per gram of soft tissue, derived from untreated, GSK2656157-treated, or GSK2656157 + Asn–treated mice ($n = 5$ per group) after subcutaneous infection. Mann-Whitney *U* test, *$P < 0.05$; **$P < 0.01$. (**C**) Representative pictures of the spleens isolated at day 8 after infection from the indicated groups of mice in (B) are shown.

mice 8 days after infection were similar to those of infected and untreated mice (Fig. 5C). Furthermore, mice administered with asparagine lost the protective effect of ISRIB (fig. S5C). These results, together, demonstrate that both GSK2656157 and ISRIB act in vivo to inhibit the reprogramming of asparagine metabolism by GAS, which is essential for its pathogenesis.

GSK2656157 and ISRIB affect chemokine and cytokine response

To gain an initial understanding of the effect of GSK2656157 and ISRIB treatments on chemokine and cytokine response, we assessed the amounts of macrophage inflammatory protein 2 (MIP-2), interleukin-1β (IL-1β), and IL-6 in soft tissue biopsies of mice. These immune mediators were implicated in tissue destruction during GAS invasive infections (*46*–*50*). We found that, in infected and untreated mice, MIP-2 amounts appeared the highest on day 6 after infection and declined to ~15% of their maximal amount on day 8. In GSK2656157-treated mice, MIP-2 amounts were significantly lower ($P = 0.0079$) on days 4 and 6 after infection and, on day 8 PI, sharply declined and became negligible (Fig. 6A). The administration of asparagine reverted MIP-2 amounts in GSK2656157-treated mice to that observed in untreated mice. IL-1β and IL-6 release trends were similar to those found for MIP-2 (Fig. 6, B and C). Like GSK2656157, ISRIB treatment decreased MIP-2, IL-1β, and IL-6 amounts, and its inhibitory effects were negated by providing mice with asparagine (fig. S6, A to C). These results demonstrate that an increased pro-inflammatory immune response from the host directly coincides with its ability to produce and supply GAS with asparagine during NF infection.

A therapeutic time window for post-infection treatment against GAS with ISRIB or GSK2656157

Because the diagnosis of NF at its early stages is far from trivial as symptoms can be ambiguous (*51*), we tested whether the treatment with ISRIB or GSK2656157 would be effective when given after infection. To this end, we enumerated and compared soft tissue CFUs in three groups of mice, all of which were subcutaneously infected with 5×10^6 CFU of strain JS14. Group 1 (control) was treated with vehicle only [90% saline, 5% polyethylene glycol (PEG), and 5% dimethyl sulfoxide (DMSO)]. Group 2 was pretreated subcutaneously with ISRIB 4 hours before bacterial infection, after which subcutaneous and intraperitoneal injections were given alternately every 12 hours until the sixth day. Group 3 was treated with ISRIB only 12 hours after infection, after which subcutaneous and intraperitoneal injections were given alternately every 12 hours until the sixth day. Pretreatment with ISRIB facilitated the reduction of soft tissue CFUs by about 10^3-fold on day 9 and more than 10^6-fold on day 11 after infection than in the control group of mice (Fig. 7A). ISRIB treatment given after infection (group 3) enhanced GAS clearance by two to three orders of magnitude on days 9 and 11, compared to the control group (Fig. 7A). Both ISRIB pre-infection and post-infection administration had similar marked effects on lesion size progression and wound appearance. Lesions of treated mice were considerably smaller as observed already on day 2 after infection, suggesting that the wound healing process in ISRIB-treated mice was accelerated (Fig. 7, B and C). Similar results were obtained using GSK2656157 for pre- or post-treatment (fig. S7, A to C). These data indicate that ISRIB and GSK2656157 can cure NF in the murine model.

DISCUSSION

Host-directed therapies are a relatively new and promising approach for treating infectious diseases (*52*). Drugs targeting host processes may largely avoid the development of bacterial antibiotic resistance. However, these drugs may also have a generally increased risk for side effects by tilting the immune response toward collateral damage. We did not observe this for PERK inhibitors and ISRIB in the murine model of human soft tissue infection. Nevertheless, the approval of PERK inhibitors and ISRIB for human use is still being assessed.

Previously, we showed that GAS increases asparagine availability by inducing ER stress, which up-regulates the transcription of asparagine synthetase in the infected host cell. Because GAS uses asparagine to alter its gene expression and control its proliferation rate (*22*), the goals of the present investigation were to decipher the precise signaling pathway that GAS uses to obtain asparagine from the host and test the effectiveness of inhibitors of this pathway as treatments against invasive GAS infections.

Asparagine synthetase basal activity in mammalian cells and tissues is usually low. However, ATF4 strongly up-regulates asparagine synthetase transcription by binding to an enhancer element located in the corresponding gene promoter region (*53*). Here, we provide pharmacological evidence that UPR, through its PERK-eIF2α-ATF4

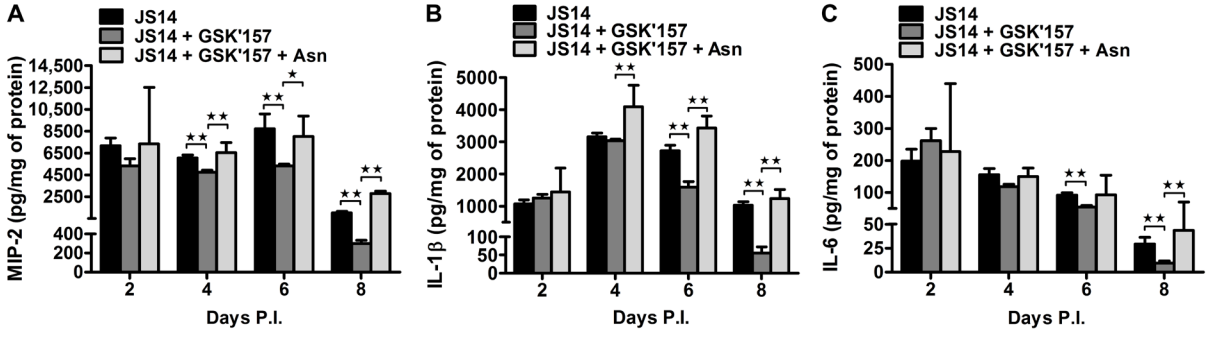

Fig. 6. GSK2656157 lowers the amount of lesional pro-inflammatory mediators. BALB/c mice were infected by subcutaneous administration of 5×10^6 CFU (a sublethal dose) of strain JS14 and were then either untreated or treated with GSK2656157 or with GSK2656157 + Asn. (**A** to **C**) MIP-2 (A), IL-1β (B), and IL-6 (C) (pg/mg protein) in skin lesions of infected mice untreated or treated with GSK2656157 or with GSK2656157 + Asn ($n = 5$ per group). Assays by ELISA were conducted in duplicate. Data are means ± SD. Mann-Whitney *U* test, $^*P < 0.05$; $^{**}P < 0.01$.

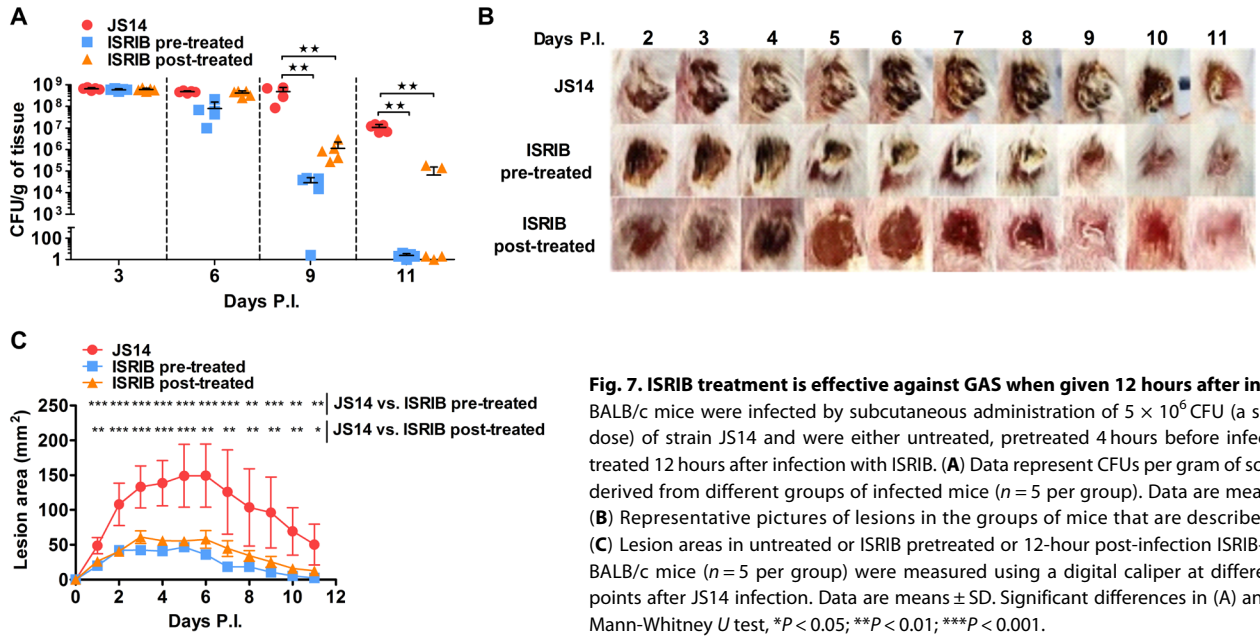

Fig. 7. ISRIB treatment is effective against GAS when given 12 hours after infection. BALB/c mice were infected by subcutaneous administration of 5×10^6 CFU (a sublethal dose) of strain JS14 and were either untreated, pretreated 4 hours before infection, or treated 12 hours after infection with ISRIB. (**A**) Data represent CFUs per gram of soft tissue derived from different groups of infected mice ($n = 5$ per group). Data are means ± SD. (**B**) Representative pictures of lesions in the groups of mice that are described in (A). (**C**) Lesion areas in untreated or ISRIB pretreated or 12-hour post-infection ISRIB–treated BALB/c mice ($n = 5$ per group) were measured using a digital caliper at different time points after JS14 infection. Data are means ± SD. Significant differences in (A) and (C) by Mann-Whitney *U* test, $^*P < 0.05$; $^{**}P < 0.01$; $^{***}P < 0.001$.

pathway, serves as the main arm of the ISR for inducing asparagine synthetase during GAS infection. The specific PERK inhibitors (GSK2606414 and GSK2656157) and ISRIB inhibited asparagine formation in various mammalian cells and in a murine human soft tissue GAS infection model. The inhibition was achieved in mammalian cells in a dose- and time-dependent manner, and exogenously added asparagine annulled the inhibitory effect. Furthermore, we observed that GAS did not activate other UPR signaling branches (IRE1 and ATF6). Our results show that GAS explicitly targets the PERK-eIF2α-ATF4 pathway to obtain asparagine from the host, and this process can be blocked by inhibitors acting along the signaling pathway axis.

Neutrophils are an essential part of the host's primary innate immune defense against GAS infections (*13*, *44*). NF characteristics are rapidly spreading inflammation and subsequent necrosis of the fascial planes and surrounding subcutaneous tissue. Histologically, NF is characterized by the destruction of soft tissue, a paucity of infiltrating neutrophils to the leading infection site where many Gram-positive cocci microcolonies are present (*15*, *21*). The comparative immunohistological study of soft tissue from GSK2656157-treated and untreated bacteria-infected mice showed that, on days 2 and 4 after infection, GSK2656157-treated mice displayed a substantially enhanced neutrophil infiltration into the fascial zone filled with GAS bacteria. However, on day 2, the amounts of MIP-2 were similar in both groups of mice.

Furthermore, on day 4, there was only a slight reduction in MIP-2 in GSK2656157-treated mice. These findings demonstrate that MIP-2 was not the limiting factor accountable for the difference in the ability of neutrophils to migrate to the site of infection. Neutrophil migration into infected and inflamed soft tissue is a complex process affected by multiple signals generated during the invasion of bacteria into sterile tissue sites (*54*). In addition, the infection microenvironment may affect neutrophil lifespan, and with increased longevity, neutrophils can perform additional protective functions like modulation of downstream adaptive immune responses or inflammation resolution through anti-inflammatory signaling (*54*). GSK2656157 and ISRIB affect GAS virulence and proliferation rate, thus probably changing the infection microenvironment, perhaps making the bacteria more susceptible to killing by neutrophils. The ratio between bacteria and neutrophils in the tissue is critical for infection outcomes (*55*).

Successful host defense in GAS soft tissue infection requires a precise balance between the immune response and inflammation to avoid collateral host tissue damage, which may exacerbate the infection. Exaggerated inflammation is a hallmark of GAS invasive diseases. Several studies, including a dual RNA sequencing analysis, demonstrated that chemokines like IL-8 and cytokines such as IL-1β and IL-6 are strongly up-regulated during GAS soft tissue infections (*46*, *50*, *56*–*58*). Here, we show that GSK2656157 and ISRIB reduce the extent of the pro-inflammatory signals in a time-dependent manner. Histopathological analyses showed that soft tissue of GSK2656157-treated mice started healing by days 4 to 8 after infection. However, the soft tissue from control mice was heavily damaged. Thus, it is conceivable that, by increasing the GAS rate of multiplication and altering its expression of virulence factors, asparagine stimulates the host pro-inflammatory response, leading to tissue damage associated with GAS NF.

It has been demonstrated that streptolysin S activates nociceptor neurons and produces pain during infection. Nociceptors release the neuropeptide calcitonin gene–related peptide (CGRP) into infected tissues, inhibiting neutrophil recruitment and the opsonophagocytic killing of GAS (*59*). CGRP is produced by the adrenomedullin 2 (ADM2) gene product that is proteolytically processed to biologically active multifunctional peptides (*60*). ATF4 controls the transcription of the *ADM2* gene under ISR conditions, and this process can be blocked by ISRIB (*61*). Thus, we believe that ISRIB will alleviate the GAS pain response, further facilitating neutrophil recruitment for host defense.

The existence of a therapeutic window of time for treatment of GAS NF is critical (*8*, *10*, *13*, *15*, *16*). We showed that treatment of infected mice with ISRIB or GSK2656157 12 hours after infection successfully terminated the infection. Thus, it is reasonable to assume

that subcutaneous injection of 5×10^6 GAS CFU to 10- to 12-g mice tilts the balance between host defense and GAS virulence in favor of the latter. Nevertheless, ISRIB or GSK2656157 treatments are still valid at 12 hours after infection, suggesting that analogous compounds may be valuable in clearing GAS human infections either alone or in combination with antibiotics and surgery.

In conclusion, UPR signaling plays an essential role in the multiplication and rapid spread of GAS from the skin into the fascia by inducing host-mediated asparagine release. Here, we show that preventing asparagine release using PERK and ISR inhibitors slowed infection progression in a murine model of human NF and led to clearance of the infection. Furthermore, the inhibitors' administration may also be used as an adjunctive treatment to surgical debridement of infected tissue and antibiotic administration. In summary, we suggest that repurposing of host-directed drugs is a worthwhile avenue of clinical exploration to improve patient outcomes in severe GAS infections where mortality is high despite conventional prompt treatments.

MATERIALS AND METHODS

Study design

Our previous study's findings showed that GAS causes ER stress upon adherence to host cells, resulting in the up-regulation of asparagine synthetase and increased asparagine production. In the current study, we set out to identify the UPR signaling pathway involved in the GAS-induced generation of asparagine and to assess the efficacy of pathway inhibitors to cure GAS infection in a murine model of human NF. On the basis of earlier reports showing ATF4-mediated asparagine release by the host cells, in vitro experiments such as fluorescence-activated cell sorting (FACS), real-time reverse transcription polymerase chain reaction (RT-PCR), and Western blotting were performed to explore the role of the PERK-eIF2α-ATF4 axis in GAS pathogenesis and to rule out the involvement of other arms of UPR signaling pathways using various pharmacological inhibitors. GSK2606414/GSK2656157 (PERK inhibitors) and ISRIB (ISR inhibitor) were used to block the PERK-eIF2α-ATF4 pathway and, consequently, asparagine release by mammalian cells. Inhibition of asparagine release was determined through *sil* activation and rates of bacterial proliferation.

Female BALB/c OlaHsd mice, aged 3 to 4 weeks, were used for in vivo studies to examine the therapeutic efficacy of GSK2656157 and ISRIB against GAS infection. Groups of subcutaneously GAS-infected mice were either treated or untreated with inhibitors to evaluate survival, bacterial loads in tissue and spleen, lesion profile, and immunohistological studies at various post-infection stages. The possibility of a post-infection therapeutic window was also checked by the administration of ISRIB and GSK2656157 in mice 12 hours after infection with GAS. The cohort size selection for mice experiments was decided on the basis of previous experiments performed in our laboratory.

Animals

Three- to 4-week-old female BALB/c OlaHsd mice weighing 10 to 12 g were obtained from ENVIGO RMS (Israel Ltd.). Following the Hebrew University of Jerusalem's ethical guidelines, all procedures were performed for humane handling, care, and treatment of research animals (protocol number MD-18-15522-5). Mice were kept in disposable cages supplemented with enrichment, sterile regular food, water, and air supplied separately in each cage. All cages were placed in specific pathogen–free (SPF) conditions during the experiment with controlled environmental conditions. The mice were left to acclimatize for 3 days, after which treatment groups of mice were randomized, and the littermates were evenly distributed in cages. Identification markings and shaving on dorsal flanks of already weighed mice were performed, and mice were infected. After infection, mice were given wet food and monitored based on various parameters like body weight, activity, and fur and eye appearance twice a day. As per the guidelines of the Institutional Animal Care Units of the Hebrew University's School of Medicine, based on the parameters mentioned above, a scoring method was implemented to decide humane endpoints where mice were euthanized according to ethically approved procedures.

In vivo soft tissue model

The murine model of human soft tissue infection with a lethal dose of bacteria was performed to determine mice survival, as detailed previously (*21*, *47*). Briefly, GAS strains were cultured in THY medium at 37°C and grown to OD_{600} (optical density at 600 nm) = 0.3 to 0.4. Bacteria were then washed twice with sterile phosphate-buffered saline (PBS) and brought to a concentration of 1.5×10^8 CFU (JS14) or 2.5×10^8 CFU (5448) in 100 μl, injected subcutaneously into the rear flank of mice. The actual bacterial inoculum was confirmed by counting CFU on blood agar plates of serially diluted final suspension. GSK2656157 (0.1 mg per mouse per injection) or ISRIB (35 μg per mouse per injection) was administered subcutaneously 4 hours before bacterial infection, after which subcutaneous and intraperitoneal injections of the inhibitors were given alternately every 12 hours after infection until the sixth day. Mice were monitored twice a day, and Kaplan-Meier survival curves were generated and analyzed for statistical significance using the log-rank test.

The efficacy of GSK2656157 and ISRIB against GAS infection was tested on mice injected with a sublethal dose (5×10^6 CFU) of GAS strain JS14 or 5448. Different groups of mice received 100 μl of subcutaneous or intraperitoneal injections of GSK2656157 (0.1 mg per mouse per injection) or ISRIB (35 μg per mouse per injection), asparagine (2.4 mg per mouse per injection), or vehicle (DMSO:PEG 400, 1:1) twice a day for 6 days. In the post-treatment mice experiment, GSK2656157/ISRIB was injected subcutaneously 12 hours after infection, followed by intraperitoneal and subcutaneous injections of GSK2656157/ISRIB alternately every 12 hours until the sixth day.

GAS (5448 or JS14) was grown as mentioned above for the CFU enumeration in skin and spleen samples. Mice were infected on the rear flank with a GAS sublethal dose and treated with GSK2656157 (0.1 mg per mouse per injection) or ISRIB (35 μg per mouse per injection) as mentioned above. At various time points, mice were euthanized by inhalation of isoflurane followed by cervical dislocation, and skin and spleen samples were collected. Skin tissue from the injection site was collected using a punch biopsy tool (Acu-Punch, Acuderm Inc.), and spleen samples were excised and transferred to 2-ml Eppendorf tubes containing 0.5 ml of sterile PBS. Tissues were homogenized, diluted, and plated on blood agar plates, and CFUs were counted after overnight incubation at 37°C. CFU counts were normalized to the weight of the soft tissue.

The dermonecrotic skin lesions were measured daily using a digital caliper (Bar Naor Ltd.) for the lesion area's determination. The lesion area was calculated with the following formula: $A = (\pi/2)$ (length)(width) (*59*).

Cytokine measurement

Mice were infected subcutaneously with 5×10^6 CFU of JS14 in 100 μl of sterile PBS on the rear flank. In addition, different groups of mice received 100 μl of subcutaneous or intraperitoneal injections of GSK2656157, ISRIB, or vehicle, as mentioned above. After GAS infection, mice were euthanized at indicated times, and soft tissue samples surrounding the lesion were harvested by punch biopsy. The samples were minced with scissors and homogenized in lysis buffer containing 10 mM tris-HCl (pH 7.8), supplemented with 1% NP-40, 150 mM NaCl, 40 mM EDTA, and cOmplete, Mini, EDTA-free protease inhibitor cocktail tablet. The tissue samples were vortexed for 1 hour at room temperature and centrifuged at 17,000*g* for 5 min. Supernatants containing chemokines and cytokines were collected and stored at −80°C. According to the manufacturer's protocol, the amounts of chemokine MIP-2 and the pro-inflammatory cytokines IL-1β and 1L-6 were quantified using Quantikine enzyme-linked immunosorbent assay (ELISA) kits (R&D Systems). The amounts of chemokine and cytokine were normalized to the corresponding samples' total protein content, measured by Bradford protein assay (Bio-Rad Laboratories).

Statistical analysis

Statistical analysis was performed, and results were plotted using GraphPad Prism version 5 software. All values were represented as means ± SD/SEM. Data in bar graphs were analyzed by one-way analysis of variance (ANOVA) with Tukey post-test unless specified. Where indicated, the nonparametric Mann-Whitney *U* test and parametric unpaired one-tailed *t* test were used to analyze data. In all figures, *P* values were calculated to confirm the significance as follows: $*P < 0.05$; $**P < 0.01$; $***P < 0.001$. For further details of statistical analysis, please refer to table S1.

SUPPLEMENTARY MATERIALS

stm.sciencemag.org/cgi/content/full/13/605/eabd7465/DC1
Materials and methods
Figs. S1 to S7
Tables S1 to S4
Data file S1

View/request a protocol for this paper from *Bio-protocol*.

REFERENCES AND NOTES

1. A. L. Bisno, D. L. Stevens, Streptococcal infections of skin and soft tissues. *N. Engl. J. Med.* **334**, 240–246 (1996).
2. A. Efstratiou, T. Lamagni, *Epidemiology of Streptococcus pyogenes* in *Streptococcus pyogenes: Basic Biology to Clinical Manifestations,* J. J. Ferretti, D. L. Stevens, V. A. Fischetti, Eds. (University of Oklahoma Health Sciences Center, 2016).
3. D. Metzgar, A. Zampolli, The M protein of group A streptococcus is a key virulence factor and a clinically relevant strain identification marker. *Virulence* **2**, 402–412 (2011).
4. R. K. Aziz, M. Kotb, Rise and persistence of global M1T1 clone of *Streptococcus pyogenes*. *Emerg. Infect. Dis.* **14**, 1511–1517 (2008).
5. N. N. Lynskey, E. Jauneikaite, H. K. Li, X. Zhi, C. E. Turner, M. Mosavie, M. Pearson, M. Asai, L. Lobkowicz, J. Y. Chow, J. Parkhill, T. Lamagni, V. J. Chalker, S. Sriskandan, Emergence of dominant toxigenic M1T1 *Streptococcus pyogenes* clone during increased scarlet fever activity in England: A population-based molecular epidemiological study. *Lancet Infect. Dis.* **19**, 1209–1218 (2019).
6. G. E. Nelson, T. Pondo, K. A. Toews, M. M. Farley, M. L. Lindegren, R. Lynfield, D. Aragon, S. M. Zansky, J. P. Watt, P. R. Cieslak, K. Angeles, L. H. Harrison, S. Petit, B. Beall, C. A. Van Beneden, Epidemiology of invasive group A streptococcal infections in the United States, 2005–2012. *Clin. Infect. Dis.* **63**, 478–486 (2016).
7. J. R. Carapetis, A. C. Steer, E. K. Mulholland, M. Weber, The global burden of group A streptococcal diseases. *Lancet Infect. Dis.* **5**, 685–694 (2005).
8. J. N. Cole, T. C. Barnett, V. Nizet, M. J. Walker, Molecular insight into invasive group A streptococcal disease. *Nat. Rev. Microbiol.* **9**, 724–736 (2011).
9. M. W. Cunningham, Rheumatic fever, autoimmunity, and molecular mimicry: The streptococcal connection. *Int. Rev. Immunol.* **33**, 314–329 (2014).
10. R. J. Olsen, J. M. Musser, Molecular pathogenesis of necrotizing fasciitis. *Annu. Rev. Pathol.* **5**, 1–31 (2010).
11. A. P. Ralph, J. R. Carapetis, Group a streptococcal diseases and their global burden. *Curr. Top. Microbiol. Immunol.* **368**, 1–27 (2013).
12. A. C. Steer, T. Lamagni, N. Curtis, J. R. Carapetis, Invasive group a streptococcal disease: Epidemiology, pathogenesis and management. *Drugs* **72**, 1213–1227 (2012).
13. M. J. Walker, T. C. Barnett, J. D. McArthur, J. N. Cole, C. M. Gillen, A. Henningham, K. S. Sriprakash, M. L. Sanderson-Smith, V. Nizet, Disease manifestations and pathogenic mechanisms of group A streptococcus. *Clin. Microbiol. Rev.* **27**, 264–301 (2014).
14. T. C. Barnett, A. C. Bowen, J. R. Carapetis, The fall and rise of group A *Streptococcus* diseases. *Epidemiol. Infect.* **147**, 1–6 (2018).
15. D. L. Stevens, A. E. Bryant, Necrotizing soft-tissue infections. *N. Engl. J. Med.* **377**, 2253–2265 (2017).
16. U. Allen, D. Moore, Invasive group A streptococcal disease: Management and chemoprophylaxis. *Can. J. Infect. Dis. Med. Microbiol.* **21**, 115–118 (2010).
17. H. D. Davies, A. McGeer, B. Schwartz, K. Green, D. Cann, A. E. Simor, D. E. Low; Ontario Group A Streptococcal Study Group, Invasive group A streptococcal infections in Ontario, Canada. *N. Engl. J. Med.* **335**, 547–554 (1996).
18. M. Sheel, N. J. Moreland, J. D. Fraser, J. Carapetis, Development of group A streptococcal vaccines: An unmet global health need. *Expert Rev. Vaccines* **15**, 227–238 (2016).
19. J. Vekemans, F. Gouvea-Reis, J. H. Kim, J. L. Excler, P. R. Smeesters, K. L. O'Brien, C. A. Van Beneden, A. C. Steer, J. R. Carapetis, D. C. Kaslow, The path to group A *Streptococcus* vaccines: World Health Organization research and development technology roadmap and preferred product characteristics. *Clin. Infect. Dis.* **69**, 877–883 (2019).
20. A. E. Moses, S. Goldberg, Z. Korenman, M. Ravins, E. Hanski, M. Shapiro, Invasive group a streptococcal infections, Israel. *Emerg. Infect. Dis.* **8**, 421–426 (2002).
21. C. Hidalgo-Grass, M. Dan-Goor, A. Maly, Y. Eran, L. A. Kwinn, V. Nizet, M. Ravins, J. Jaffe, A. Peyser, A. E. Moses, E. Hanski, Effect of a bacterial pheromone peptide on host chemokine degradation in group A streptococcal necrotising soft-tissue infections. *Lancet* **363**, 696–703 (2004).
22. M. Baruch, I. Belotserkovsky, B. B. Hertzog, M. Ravins, E. Dov, K. S. McIver, Y. S. Le Breton, Y. Zhou, C. Y. Cheng, E. Hanski, An extracellular bacterial pathogen modulates host metabolism to regulate its own sensing and proliferation. *Cell* **156**, 97–108 (2014).
23. E. Fessler, E. M. Eckl, S. Schmitt, I. A. Mancilla, M. F. Meyer-Bender, M. Hanf, J. Philippou-Massier, S. Krebs, H. Zischka, L. T. Jae, A pathway coordinated by DELE1 relays mitochondrial stress to the cytosol. *Nature* **579**, 433–437 (2020).
24. X. Guo, G. Aviles, Y. Liu, R. Tian, B. A. Unger, Y. T. Lin, A. P. Wiita, K. Xu, M. A. Correia, M. Kampmann, Mitochondrial stress is relayed to the cytosol by an OMA1-DELE1-HRI pathway. *Nature* **579**, 427–432 (2020).
25. H. P. Harding, Y. Zhang, H. Zeng, I. Novoa, P. D. Lu, M. Calfon, N. Sadri, C. Yun, B. Popko, R. Paules, D. F. Stojdl, J. C. Bell, T. Hettmann, J. M. Leiden, D. Ron, An integrated stress response regulates amino acid metabolism and resistance to oxidative stress. *Mol. Cell* **11**, 619–633 (2003).
26. K. Zhang, R. J. Kaufman, From endoplasmic-reticulum stress to the inflammatory response. *Nature* **454**, 455–462 (2008).
27. P. Walter, D. Ron, The unfolded protein response: From stress pathway to homeostatic regulation. *Science* **334**, 1081–1086 (2011).
28. M. N. Balasubramanian, E. A. Butterworth, M. S. Kilberg, Asparagine synthetase: Regulation by cell stress and involvement in tumor biology. *Am. J. Physiol. Endocrinol. Metab.* **304**, E789–E799 (2013).
29. H. P. Harding, I. Novoa, Y. Zhang, H. Zeng, R. Wek, M. Schapira, D. Ron, Regulated translation initiation controls stress-induced gene expression in mammalian cells. *Mol. Cell* **6**, 1099–1108 (2000).
30. J. M. Axten, S. P. Romeril, A. Shu, J. Ralph, J. R. Medina, Y. Feng, W. H. Li, S. W. Grant, D. A. Heerding, E. Minthorn, T. Mencken, N. Gaul, A. Goetz, T. Stanley, A. M. Hassell, R. T. Gampe, C. Atkins, R. Kumar, Discovery of GSK2656157: An optimized PERK inhibitor selected for preclinical development. *ACS Med. Chem. Lett.* **4**, 964–968 (2013).
31. C. Sidrauski, A. M. McGeachy, N. T. Ingolia, P. Walter, The small molecule ISRIB reverses the effects of eIF2α phosphorylation on translation and stress granule assembly. *eLife* **4**, e05033 (2015).
32. A. F. Zyryanova, F. Weis, A. Faille, A. A. Alard, A. Crespillo-Casado, Y. Sekine, H. P. Harding, F. Allen, L. Parts, C. Fromont, P. M. Fischer, A. J. Warren, D. Ron, Binding of ISRIB reveals a regulatory site in the nucleotide exchange factor eIF2B. *Science* **359**, 1533–1536 (2018).
33. E. L. Abbot, W. D. Smith, G. P. Siou, C. Chiriboga, R. J. Smith, J. A. Wilson, B. H. Hirst, M. A. Kehoe, Pili mediate specific adhesion of *Streptococcus pyogenes* to human tonsil and skin. *Cell. Microbiol.* **9**, 1822–1833 (2007).
34. B. B. Hertzog, Y. Kaufman, D. Biswas, M. Ravins, P. Ambalavanan, R. Wiener, V. Angeli, S. L. Chen, E. Hanski, A sub-population of group A *Streptococcus* elicits a population-wide

production of bacteriocins to establish dominance in the host. *Cell Host Microbe* **23**, 312–323.e6 (2018).
35. I. Papandreou, N. C. Denko, M. Olson, H. Van Melckebeke, S. Lust, A. Tam, D. E. Solow-Cordero, D. M. Bouley, F. Offner, M. Niwa, A. C. Koong, Identification of an Ire1alpha endonuclease specific inhibitor with cytotoxic activity against human multiple myeloma. *Blood* **117**, 1311–1314 (2011).
36. T. Okada, K. Haze, S. Nadanaka, H. Yoshida, N. G. Seidah, Y. Hirano, R. Sato, M. Negishi, K. Mori, A serine protease inhibitor prevents endoplasmic reticulum stress-induced cleavage but not transport of the membrane-bound transcription factor ATF6. *J. Biol. Chem.* **278**, 31024–31032 (2003).
37. A. Shrivastava, A. A. Khan, M. Khurshid, M. A. Kalam, S. K. Jain, P. K. Singhal, Recent developments in L-asparaginase discovery and its potential as anticancer agent. *Crit. Rev. Oncol. Hematol.* **100**, 1–10 (2016).
38. K. S. McIver, Stand-alone response regulators controlling global virulence networks in *Streptococcus pyogenes*. *Contrib. Microbiol.* **16**, 103–119 (2009).
39. L. L. Hause, K. S. McIver, Nucleotides critical for the interaction of the *Streptococcus pyogenes* Mga virulence regulator with Mga-regulated promoter sequences. *J. Bacteriol.* **194**, 4904–4919 (2012).
40. E. R. Hondorp, K. S. McIver, The Mga virulence regulon: Infection where the grass is greener. *Mol. Microbiol.* **66**, 1056–1065 (2007).
41. M. W. Cunningham, Pathogenesis of group A streptococcal infections. *Clin. Microbiol. Rev.* **13**, 470–511 (2000).
42. H. R. Frost, M. Sanderson-Smith, M. Walker, A. Botteaux, P. R. Smeesters, Group A streptococcal M-like proteins: From pathogenesis to vaccine potential. *FEMS Microbiol. Rev.* **42**, 193–204 (2018).
43. M. J. Kim, M. N. Kim, S. H. Min, D. S. Ham, J. W. Kim, K. H. Yoon, K. S. Park, H. S. Jung, Specific PERK inhibitors enhanced glucose-stimulated insulin secretion in a mouse model of type 2 diabetes. *Metabolism* **97**, 87–91 (2019).
44. J. M. Voyich, J. M. Musser, F. R. DeLeo, *Streptococcus pyogenes* and human neutrophils: A paradigm for evasion of innate host defense by bacterial pathogens. *Microbes Infect.* **6**, 1117–1123 (2004).
45. A. E. Bryant, C. R. Bayer, R. Y. Chen, P. H. Guth, R. J. Wallace, D. L. Stevens, Vascular dysfunction and ischemic destruction of tissue in *Streptococcus pyogenes* infection: The role of streptolysin O-induced platelet/neutrophil complexes. *J. Infect. Dis.* **192**, 1014–1022 (2005).
46. V. Castiglia, A. Piersigilli, F. Ebner, M. Janos, O. Goldmann, U. Dambock, A. Kroger, S. Weiss, S. Knapp, A. M. Jamieson, C. Kirschning, U. Kalinke, B. Strobl, M. Muller, D. Stoiber, S. Lienenklaus, P. Kovarik, Type I interferon signaling prevents IL-1β-driven lethal systemic hyperinflammation during invasive bacterial infection of soft tissue. *Cell Host Microbe* **19**, 375–387 (2016).
47. C. Hidalgo-Grass, I. Mishalian, M. Dan-Goor, I. Belotserkovsky, Y. Eran, V. Nizet, A. Peled, E. Hanski, A streptococcal protease that degrades CXC chemokines and impairs bacterial clearance from infected tissues. *EMBO J.* **25**, 4628–4637 (2006).
48. C. N. LaRock, J. Todd, D. L. LaRock, J. Olson, A. J. O'Donoghue, A. A. Robertson, M. A. Cooper, H. M. Hoffman, V. Nizet, IL-1β is an innate immune sensor of microbial proteolysis. *Sci. Immunol.* **1**, eaah3539 (2016).
49. D. L. Stevens, Streptococcal toxic shock syndrome associated with necrotizing fasciitis. *Annu. Rev. Med.* **51**, 271–288 (2000).
50. T. C. Weng, C. C. Chen, H. S. Toh, H. J. Tang, Ibuprofen worsens *Streptococcus pyogenes* soft tissue infections in mice. *J. Microbiol. Immunol. Infect.* **44**, 418–423 (2011).
51. D. A. Anaya, E. P. Dellinger, Necrotizing soft-tissue infection: Diagnosis and management. *Clin. Infect. Dis.* **44**, 705–710 (2007).
52. S. H. E. Kaufmann, A. Dorhoi, R. S. Hotchkiss, R. Bartenschlager, Host-directed therapies for bacterial and viral infections. *Nat. Rev. Drug Discov.* **17**, 35–56 (2018).
53. C. L. Lomelino, J. T. Andring, R. McKenna, M. S. Kilberg, Asparagine synthetase: Function, structure, and role in disease. *J. Biol. Chem.* **292**, 19952–19958 (2017).
54. E. Kolaczkowska, P. Kubes, Neutrophil recruitment and function in health and inflammation. *Nat. Rev. Immunol.* **13**, 159–175 (2013).
55. S. C. Silverstein, R. Rabadan, How many neutrophils are enough (redux, redux)? *J. Clin. Invest.* **122**, 2776–2779 (2012).
56. P. Kachro, J. M. Eraso, R. J. Olsen, L. Zhu, S. L. Kubiak, L. Pruitt, P. Yerramilli, C. C. Cantu, M. O. Saavedra, J. Pensar, J. Corander, L. Jenkins, L. Kao, A. Granillo, A. R. Porter, F. R. DeLeo, J. M. Musser, New pathogenesis mechanisms and translational leads identified by multidimensional analysis of necrotizing myositis in primates. *MBio* **11**, e03363-19 (2020).
57. R. Thänert, A. Itzek, J. Hoßmann, D. Hamisch, M. B. Madsen, O. Hyldegaard, S. Skrede, T. Bruun, A. Norrby-Teglund; INFECT study group, E. Medina, Molecular profiling of tissue biopsies reveals unique signatures associated with streptococcal necrotizing soft tissue infections. *Nat. Commun.* **10**, 3846 (2019).
58. J. A. Valderrama, A. M. Riestra, N. J. Gao, C. N. LaRock, N. Gupta, S. R. Ali, H. M. Hoffman, P. Ghosh, V. Nizet, Group A streptococcal M protein activates the NLRP3 inflammasome. *Nat. Microbiol.* **2**, 1425–1434 (2017).
59. F. A. Pinho-Ribeiro, B. Baddal, R. Haarsma, M. O'Seaghdha, N. J. Yang, K. J. Blake, M. Portley, W. A. Verri Jr., J. B. Dale, M. R. Wessels, I. M. Chiu, Blocking neuronal signaling to immune cells treats Streptococcal invasive infection. *Cell* **173**, 1083–1097.e22 (2018).
60. J. Roh, C. L. Chang, A. Bhalla, C. Klein, S. Y. Hsu, Intermedin is a calcitonin/calcitonin gene-related peptide family peptide acting through the calcitonin receptor-like receptor/receptor activity-modifying protein receptor complexes. *J. Biol. Chem.* **279**, 7264–7274 (2004).
61. I. E. Kovaleva, A. A. Garaeva, P. M. Chmakov, A. G. Evstafieva, Intermedin/adrenomedullin 2 is a stress-inducible gene controlled by activating transcription factor 4. *Gene* **590**, 177–185 (2016).

Funding: This work was supported by grants from the Israeli Science Foundation administered by the Israel Academy of Sciences and Humanities (ISF) (grant 295/17 to E.H.), the F.I.R.S.T. grant from ISF (958/20 to E.H. and B.T.), the ISF-UGC Joint Scientific Research Program (2266/15 to E.H. and A.K.J.), and the National Research Foundation, Prime Minister's Office, Singapore under its Campus of Research Excellence and Technological Enterprise (CREATE) program (to E.H.). In addition, A.A. and A.S. are thankful to the PBC Fellowship Program by the Israeli council for partial funding. **Author contributions:** E.H. and B.T. conceived the project and supervised the study; A.A., A.S., M.R., B.T., A.K.J., and E.H. conceptualized the study; A.A., A.S., M.R., and E.H. designed experiments; A.A., A.S., and M.R. developed methods; A.A., A.S., M.R., D.B., P.A., K.X.Z.L., and R.Y.M.T. conducted the investigation; A.A., A.S., M.R., D.B., and P.A. performed the analysis; A.A., A.S., M.R., B.T., and E.H. wrote the manuscript. **Competing interests:** The authors declare that they have no competing interests. **Data and materials availability:** All data associated with this study are present in the paper or the Supplementary Materials. Raw data from figures are available in data file S1.

Submitted 9 July 2020
Resubmitted 24 February 2021
Accepted 25 June 2021
Published 4 August 2021
10.1126/scitranslmed.abd7465

Citation: A. Anand, A. Sharma, M. Ravins, D. Biswas, P. Ambalavanan, K. X. Z. Lim, R. Y. M. Tan, A. K. Johri, B. Tirosh, E. Hanski, Unfolded protein response inhibitors cure group A streptococcal necrotizing fasciitis by modulating host asparagine. *Sci. Transl. Med.* **13**, eabd7465 (2021).

Science Translational Medicine

Unfolded protein response inhibitors cure group A streptococcal necrotizing fasciitis by modulating host asparagine

Aparna Anand, Abhinay Sharma, Miriam Ravins, Debabrata Biswas, Poornima Ambalavanan, Kimberly Xuan Zhen Lim, Rachel Ying Min Tan, Atul Kumar Johri, Boaz Tirosh and Emanuel Hanski

Sci Transl Med **13**, eabd7465.
DOI: 10.1126/scitranslmed.abd7465

Nixing necrosis

Group A streptococcus is one cause of flesh-eating necrotizing fasciitis. Anand *et al*. show that a branch of unfolded protein response (UPR) promotes the infection-induced increase in host cell asparagine that helps this bacterium infiltrate connective and soft tissue. Inhibiting the UPR or upstream ER stress restricted bacterial access to asparagine and protected mice against group A streptococcal infection in prophylactic and therapeutic models of necrotizing fasciitis, suggesting a strategy to treat this potentially deadly disease.